Hanuabada village, Port Moresby

Chapter 11
Papua New Guinea

The contributions of Kasis Inape from the Papua New Guinea National Weather Service and Maino Virobo from the Department of Environment and Conservation are gratefully acknowledged

Introduction

This chapter provides a brief description of Papua New Guinea, its past and present climate as well as projections for the future. The climate observation network and the availability of atmospheric and oceanic data records are outlined. The annual mean climate, seasonal cycles and the influences of large-scale climate features such as the West Pacific Monsoon and patterns of climate variability (e.g. the El Niño-Southern Oscillation) are analysed and discussed. Observed trends and analysis of air temperature, rainfall, extreme events (including tropical cyclones), sea-surface temperature, ocean acidification, mean and extreme sea levels are presented. Projections for air and sea-surface temperature, rainfall, sea level, ocean acidification and extreme events for the 21st century are provided. These projections are presented along with confidence levels based on expert judgement by Pacific Climate Change Science Program (PCCSP) scientists. The chapter concludes with a summary table of projections (Table 11.4). Important background information, including an explanation of methods and models, is provided in Chapter 1. For definitions of other terms refer to the Glossary.

11.1 Climate Summary

11.1.1 Current Climate

- Sites in Papua New Guinea have very weak seasonal variations in temperature. Sea-surface temperatures have a strong influence on average monthly air temperatures.
- The south of Papua New Guinea has a wet season from November to April and a dry season from May to October, while further north rainfall is more consistent throughout the year.
- Rainfall in Papua New Guinea is influenced by the West Pacific Monsoon. High year-to-year variability in rainfall is mostly due to the impact of the El Niño-Southern Oscillation.
- Warming trends are evident in both annual and seasonal mean air temperatures at Port Moresby for the period 1950–2009. These trends are considerably stronger in minimum air temperatures when compared to maximum air temperatures.
- Annual and seasonal rainfall trends for Port Moresby for the period 1950–2009 and Kavieng for the period 1957–2009 are not statistically significant.
- The sea-level rise near Papua New Guinea measured by satellite altimeters since 1993 is about 7 mm per year.
- On average, Port Moresby experiences six tropical cyclones per decade, with most occurring between November and April.

11.1.2 Future Climate

Over the course of the 21st century:

- Surface air temperature and sea-surface temperature are projected to continue to increase (*very high* confidence).
- Annual and seasonal mean rainfall is projected to increase (*high* confidence).
- The intensity and frequency of days of extreme heat are projected to increase (*very high* confidence).
- The intensity and frequency of days of extreme rainfall are projected to increase (*high* confidence).
- The incidence of drought is projected to decrease (*moderate* confidence).
- Tropical cyclone numbers are projected to decline in the south-west Pacific Ocean basin (0–40ºS, 130ºE –170ºE) (*moderate* confidence).
- Ocean acidification is projected to continue (*very high* confidence).
- Mean sea-level rise is projected to continue (*very high* confidence).

11.2 Country Description

Papua New Guinea consists of the eastern half of New Guinea Island and about 700 offshore islands between the equator and 12°S, and 140°E–160°E. At 462 243 km^2, Papua New Guinea is the largest of the 15 PCCSP Partner Countries. The country's geography is diverse and, in places, extremely rugged. A spine of mountains, the New Guinea Highlands, runs the length of New Guinea Island, which is mostly covered with tropical rainforest.

Dense rainforests can also be found in the lowland and coastal areas as well as the very large wetland areas surrounding the Sepik and Fly Rivers. The highest peak is Mount Wilhelm at 4697 m (Papua New Guinea Country Statistics, SOPAC, 2010).

The population of Papua New Guinea is approximately 6 744 955, with 40% living in the highlands and 18% in urban areas. The capital, Port Moresby, is located in the south-east and has a population of approximately 500 000.

Eighty-five percent of the population live a subsistence lifestyle in rural areas. These people depend on traditional agriculture and fishing for their livelihoods. Mining and oil production are the main sources of revenue for Papua New Guinea, accounting for 60% of export earnings and 20% of government revenue. Agricultural crops are still a major source of revenue, in particular copra (Papua New Guinea is the biggest producer in the South Pacific), coffee, palm oil and cocoa. Export of forestry products, once among the country's main sources of revenue, has declined in recent years.

Figure 11.1: Papua New Guinea

11.3 Data Availability

There are currently 39 operational meteorological stations in Papua New Guinea. Multiple observations within a 24-hour period are taken at 18 stations: four synoptic stations in Momase, two in the Highlands, six in the Southern region and six in the New Guinea Islands. In addition there are three single observation climate stations and 18 single observation rainfall stations. The primary climate station is located in Port Moresby (Figure 11.1). Rainfall data for Port Moresby are available from 1890, largely complete from 1905. Air temperature data are available from 1939. Madang, Wewak, Misima, Kavieng and Momote have more than 50 years of rainfall data.

Climate records for Port Moresby from 1950 and Kavieng (an island to the north-east) from 1957 (air temperature from 1962) have been used. Both records are homogeneous and more than 95% complete.

There are a number of sea-level records available for the Papua New Guinea region. The best appear to be Port Moresby II (1984–1994), Rabaul (1966–1997), Lombrum (1994–present), Lae (1984–2000), Anewa Bay (1968–1977), Kavieng (1984–1998), Madang (1984–1998), Goods Island (1989–present) and Thursday Island III (1983–2002). A global positioning system instrument to estimate vertical land motion was deployed at Manus Island in 2002 and will provide valuable direct estimates of local vertical land motion in future years. Both satellite (from 1993) and in situ sea-level data (1950–2009; termed reconstructed sea level; Volume 1, Section 2.2.2.2) are available on a global 1° x 1° grid.

Long-term locally-monitored sea-surface temperature data are unavailable for Papua New Guinea, so large-scale gridded sea-surface temperature datasets have been used (HadISST, HadSST2, ERSST and Kaplan Extended SST V2; Volume 1, Table 2.3).

Training in *Pacific Climate Futures*, Port Moresby

11.4 Seasonal Cycles

Sites in Papua New Guinea have very weak seasonal variations in temperature (Figure 11.2). Port Moresby is further south than Kavieng, so its seasonal temperature cycle is stronger with about 2.5ºC between the warmest month (November) and the coolest (July). Sea-surface temperatures have a strong influence on average monthly air temperatures.

The seasonal cycles of monthly-mean rainfall (Figure 11.2) show a wet season from November to April and a dry season from May to October. However, these seasons are only clearly different in Port Moresby, where about 78% of the yearly average rainfall comes in the wet season. The West Pacific Monsoon is responsible for most of the rainfall in Port Moresby and during the dry season Port Moresby is exposed to dry south-easterly winds. In Kavieng rainfall is more consistent year-round although the peak in rainfall corresponds to the monsoon season from December to April. Kavieng and other sites in the north of Papua New Guinea are affected by the Intertropical Convergence Zone and to a lesser extent the South Pacific Convergence Zone. They lie in the West Pacific Warm Pool, so experience convective rain throughout the year. As a result, Kavieng's average annual rainfall (3150 mm) is much higher than Port Moresby's (1190 mm).

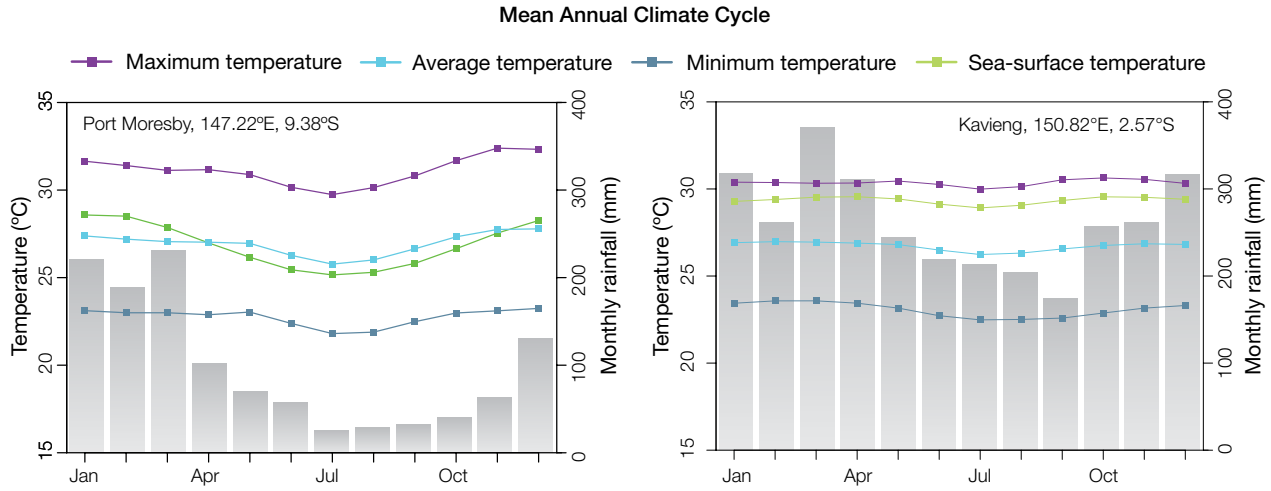

Figure 11.2: Mean annual cycle of rainfall (grey bars) and daily maximum, minimum and mean air temperatures at Port Moresby (left) and Kavieng (right), and local sea-surface temperatures derived from the HadISST dataset (Volume 1, Table 2.3).

11.5 Climate Variability

Year-to-year variability in rainfall is high in Papua New Guinea. At both Port Moresby and Kavieng the wettest years receive up to three times the rainfall of the driest years (Figure 11.4). The El Niño-Southern Oscillation (ENSO) drives much of this variability. Generally, El Niño years are drier than average while La Niña years are wetter than average. Table 11.1 shows that at Port Moresby, the dry season in El Niño years tends to be cooler than normal and warmer in La Niña years, while the wet season is cooler than normal in El Niño years. Another impact of El Niño is a late start to the monsoon season. Modoki ENSO events (Volume 1, Section 3.4.1) appear to have very similar impacts in Port Moresby to canonical ENSO events.

During El Niño events Kavieng tends to have wet seasons that are wetter than normal, and that tend to have warmer nights and cooler days. There is no clear influence of ENSO during the dry season in Kavieng.

Table 11.1: Correlation coefficients between indices of key large-scale patterns of climate variability and minimum and maximum temperatures (Tmin and Tmax) and rainfall at Port Moresby. Only correlation coefficients that are statistically significant at the 95% level are shown.

Climate feature/index		Dry season (May-October)			Wet season (November-April)		
		Tmin	Tmax	Rain	Tmin	Tmax	Rain
ENSO	Niño3.4	-0.66	-0.43		0.42	0.59	-0.51
	Southern Oscillation Index	0.65	-0.61		-0.28	-0.52	0.49
Interdecadal Pacific Oscillation Index							
ENSO Modoki Index		-0.34	-0.43			0.30	-0.29
Number of years of data		67	66	99	69	67	107

Table 11.2: Correlation coefficients between indices of key large-scale patterns of climate variability and minimum and maximum temperatures (Tmin and Tmax) and rainfall at Kavieng. Only correlation coefficients that are statistically significant at the 95% level are shown.

Climate feature/index		Dry season (May-October)			Wet season (November-April)		
		Tmin	Tmax	Rain	Tmin	Tmax	Rain
ENSO	Niño3.4				0.40	-0.38	0.34
	Southern Oscillation Index				-0.35	0.41	-0.27
Interdecadal Pacific Oscillation Index							
ENSO Modoki Index						-0.37	0.40
Number of years of data		46	44	75	45	45	73

11.6 Observed Trends

11.6.1 Air Temperature

Warming trends of a similar magnitude are evident in both annual and seasonal mean air temperatures at Port Moresby for the period 1950–2009. Air temperature trends are generally greater in the wet season than they are in the dry season and minimum air temperature trends are considerably stronger than maximum air temperatures trends (Figure 11.3 and Table 11.3).

11.6.2 Rainfall

Annual and seasonal rainfall trends for Port Moresby for the period 1950–2009 and Kavieng for the period 1957–2009 are not statistically significant (Table 11.3 and Figure 11.4).

11.6.3 Extreme Events

The tropical cyclone season in the south-eastern coastal regions of Papua New Guinea is between November and April. Occurrences outside this period are rare.
The tropical cyclone archive for the Southern Hemisphere indicates that between the 1969/70 and 2009/10 seasons, the centre of 23 tropical cyclones passed within approximately 400 km of Port Moresby (Figure 11.5). This represents an average of six cyclones per decade. Tropical cyclones were most frequent in ENSO-neutral years (eight cyclones per decade) and least frequent in El Niño and La Niña years (four cyclones per decade).

In the southern Papua New Guinea region, prolonged rainfall during La Niña events leads to serious floods and landslides. El Niño events are associated with droughts.

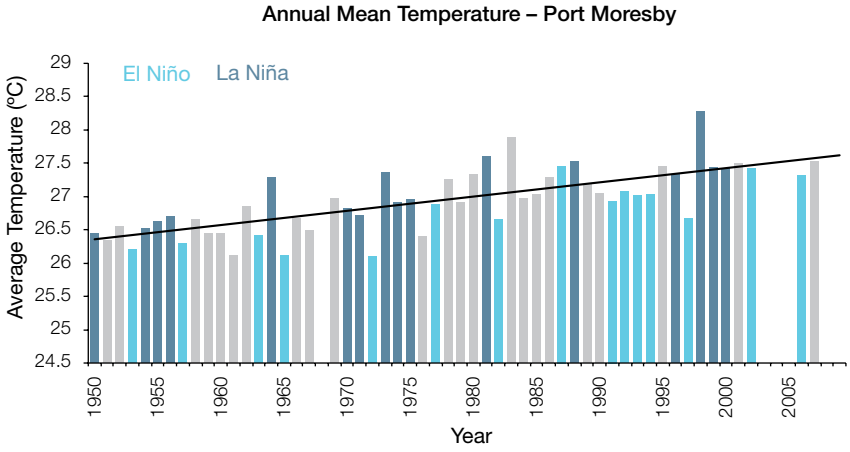

Figure 11.3: Annual mean air temperature at Port Moresby. Light blue, dark blue and grey bars denote El Niño, La Niña and neutral years respectively.

Table 11.3: Annual and seasonal trends in maximum, minimum and mean air temperature (Tmax, Tmin and Tmean) and rainfall at Port Moresby for the period 1950–2009 and rainfall only at Kavieng for the period 1957–2009. Asterisks indicate significance at the 95% level. Persistence is taken into account in the assessment of significance as in Power and Kociuba (in press). The statistical significance of the air temperature trends is not assessed.

	Port Moresby Tmax (°C per 10 yrs)	Port Moresby Tmin (°C per 10 yrs)	Port Moresby Tmean (°C per 10 yrs)	Port Moresby Rain (mm per 10 yrs)	Kavieng Rain (mm per 10 yrs)
Annual	+0.11	+0.31	+0.21	+7	-27
Wet season	+0.14	+0.32	+0.23	-4	-42
Dry season	+0.08	+0.31	+0.20	+4	+13

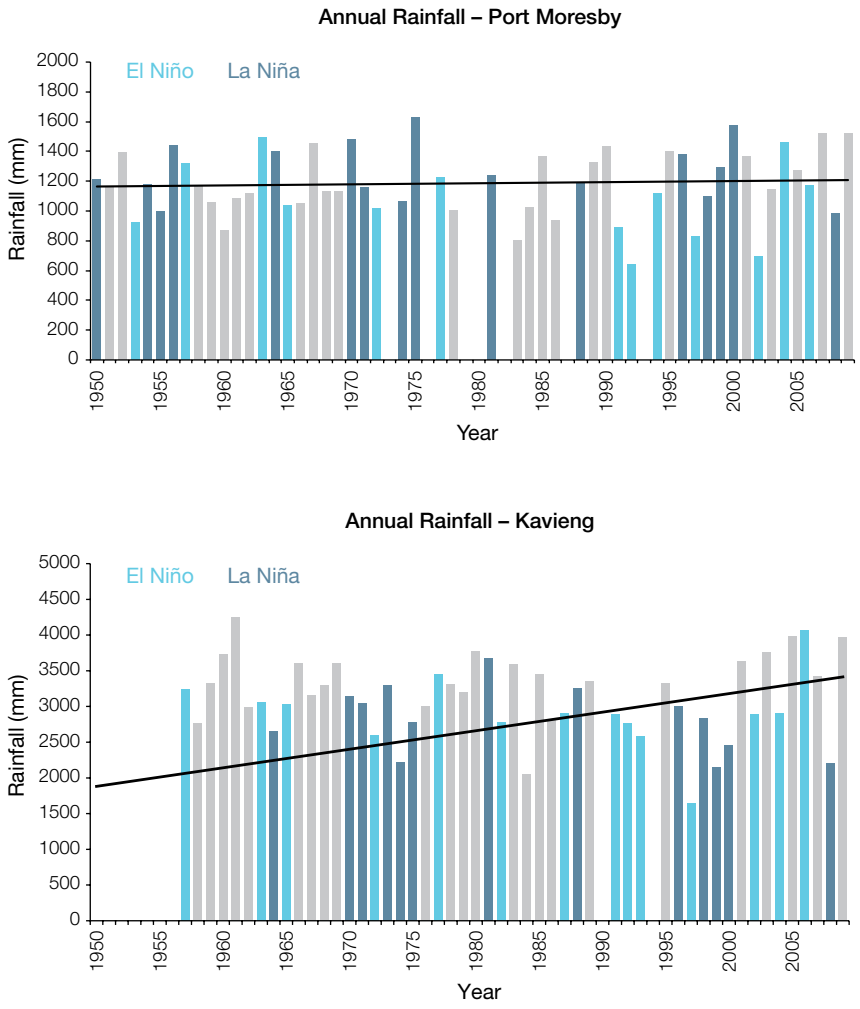

Figure 11.4: Annual rainfall at Port Moresby (top) and Kavieng (bottom). Light blue, dark blue and grey bars denote El Niño, La Niña and neutral years respectively.

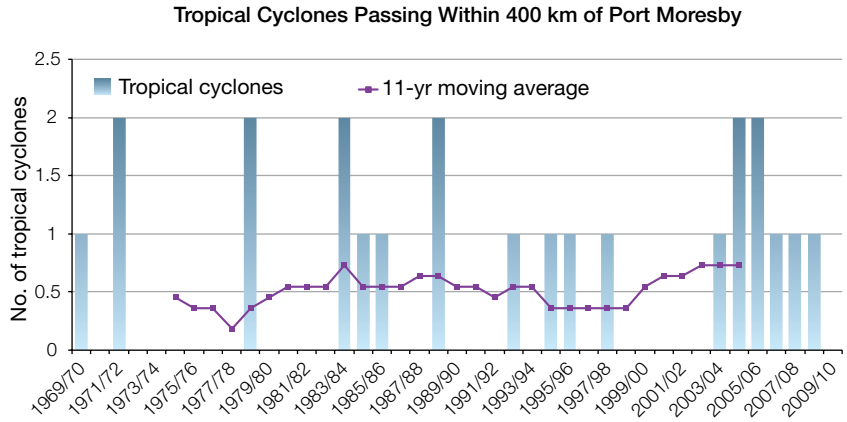

Figure 11.5: Tropical cyclones passing within 400 km of Port Moresby per season. The 11-year moving average is in purple.

11.6.4 Sea-Surface Temperature

Water temperatures in the Papua New Guinea region have risen gradually since the 1950s. Since the 1970s the rate of warming has been approximately 0.11°C per decade. Figure 11.8 shows the 1950–2000 sea-surface temperature changes (relative to a reference year of 1990) from three different large-scale sea-surface temperature gridded datasets (HadSST2, ERSST and Kaplan Extended SST V2; Volume 1, Table 2.3). At these regional scales, natural variability may play a large role in determining the sea-surface temperature making it difficult to any identify long-term trends.

11.6.5 Ocean Acidification

Based the large-scale distribution of coral reefs across the Pacific and the seawater chemistry, Guinotte et al. (2003) suggested that seawater aragonite saturation states above 4 were optimal for coral growth and for the development of healthy reef ecosystems, with values from 3.5 to 4 adequate for coral growth, and values between 3 and 3.5, marginal. Coral reef ecosystems were not found at seawater aragonite saturation states below 3 and these conditions were classified as extremely marginal for supporting coral growth.

In the Papua New Guinea region, the aragonite saturation state has declined from about 4.5 in the late 18th century to an observed value of about 3.9 ± 0.1 by 2000.

11.6.6 Sea Level

Monthly averages of the historical tide gauge, satellite (since 1993) and gridded sea-level (since 1950) data agree well after 1993 and indicate interannual variability in sea levels of about 23 cm (estimated 5–95% range) after removal of the seasonal cycle (Figure 11.10). The sea-level rise near Papua New Guinea measured by satellite altimeters (Figure 11.6) since 1993 is about 7 mm per year, larger than the global average of 3.2 ± 0.4 mm per year. This rise is partly linked to a pattern related to climate variability from year to year and decade to decade (Figure 11.10).

11.6.7 Extreme Sea-Level Events

The annual climatology of the highest daily sea levels has been evaluated from hourly measurements by tide gauges at Lombrum (Manus Province) and Rabaul (East New Britain Province) (Figure 11.7). Highest tides at both locations tend to occur around the solstices, with a higher December maximum, particularly at Rabaul. There is little seasonal cycle throughout the year but seasonal water levels at both locations are significantly higher during La Niña years and lower during El Niño years. The tidal, seasonal, and short-term components combine to create the highest likelihood for extreme water levels between November and February of La Niña years at Lombrum and November to February and April of La Niña years at Rabaul. At Lombrum, the 10 highest recorded water levels all occurred in January or early February and most occurred during La Niña years from November to February. Three events occurred from May to July of ENSO-neutral years. At Rabaul, seven of the top 10 events occurred during La Niña years and all events occurred over the period from November to March. It is important to note that the annual climatology produced by these two tide gauge locations may not be indicative of other coastal areas of Papua New Guinea, particularly the Gulf of Papua.

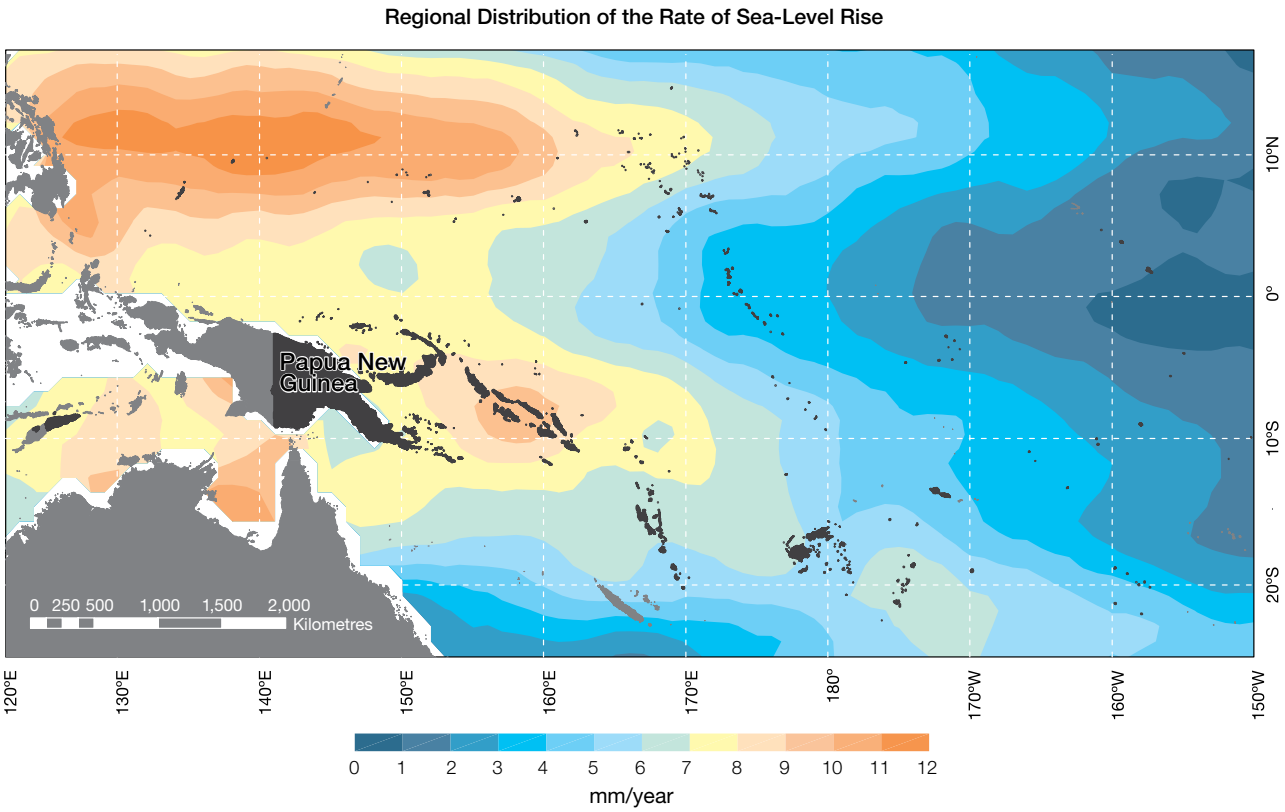

Figure 11.6: The regional distribution of the rate of sea-level rise measured by satellite altimeters from January 1993 to December 2010, with the location of Papua New Guinea indicated. Further detail about the regional distribution of sea-level rise is provided in Volume 1, Section 3.6.3.2.

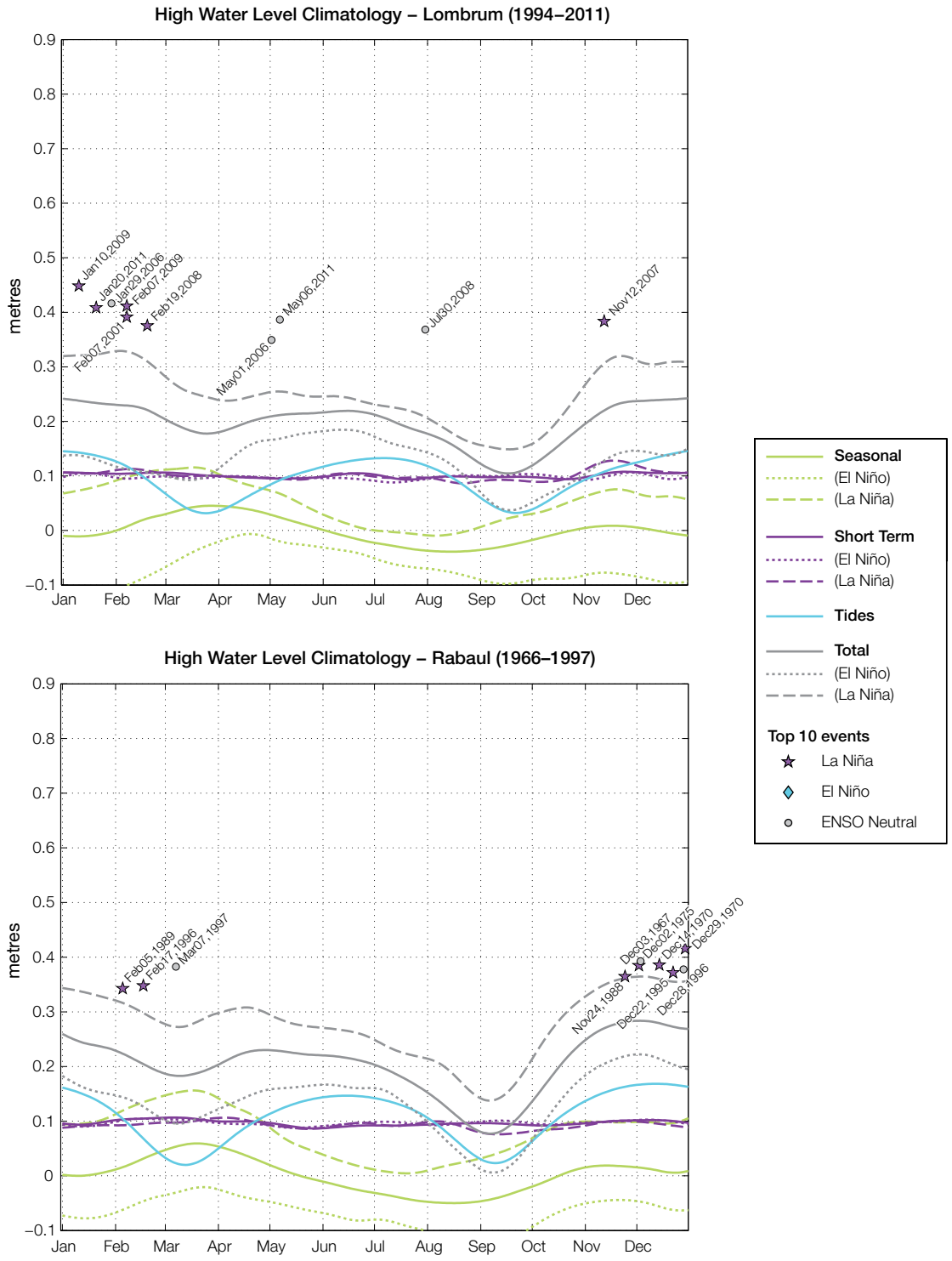

Figure 11.7: The annual cycle of high waters relative to Mean Higher High Water (MHHW) due to tides, short-term fluctuations (most likely associated with storms) and seasonal variations for Lombrum (top) and Rabaul (bottom). The tides and short-term fluctuations are respectively the 95% exceedence levels of the astronomical high tides relative to MHHW and short-term sea level fluctuations. Components computed only for El Niño and La Niña years are shown by dotted and dashed lines, and grey lines are the sum of the tide, short-term and seasonal components. The 10 highest sea level events in the record relative to MHHW are shown and coded to indicate the phase of ENSO at the time of the extreme event.

11.7 Climate Projections

Climate projections have been derived from up to 18 global climate models from the CMIP3 database, for up to three emissions scenarios (B1 (low), A1B (medium) and A2 (high)) and three 20-year periods (centred on 2030, 2055 and 2090, relative to 1990). These models were selected based on their ability to reproduce important features of the current climate (Volume 1, Section 5.2.3), so projections from each of the models are plausible representations of the future climate. This means there is not one single projected future for Papua New Guinea, but rather a range of possible futures. The full range of these futures is discussed in the following sections.

These projections do not represent a value specific to any actual location, such as a town or city in Papua New Guinea. Instead, they refer to an average change over the broad geographic region encompassing the islands of Papua New Guinea and the surrounding ocean (Figure 1.1 shows the regional boundaries). Some information regarding dynamical downscaling simulations from the CCAM model (Section 1.7.2) is also provided, in order to indicate how changes in the climate on an individual island-scale may differ from the broad-scale average.

Section 1.7 provides important information about interpreting climate model projections.

11.7.1 Temperature

Surface air temperature and sea-surface temperature are projected to continue to increase over the course of the 21st century. There is *very high* confidence in this direction of change because:

- Warming is physically consistent with rising greenhouse gas concentrations.
- All CMIP3 models agree on this direction of change.

The majority of CMIP3 models simulate a slight increase (<1°C) in annual and seasonal mean temperature by 2030, however by 2090 under the A2 (high) emissions scenario temperature increases of greater than 2.5°C are simulated by almost all models (Table 11.4). Given the close relationship between surface air temperature and sea-surface temperature, a similar (or slightly weaker) rate of warming is projected for the surface ocean (Figure 11.8). There is *high* confidence in this range and distribution of possible futures because:

- There is generally close agreement between modelled and observed temperature trends over the past 50 years in the vicinity of Papua New Guinea, although observational records are limited (Figure 11.8).

The 8 km CCAM simulations indicate considerable spatial variability in temperature change between 1990 and 2090 (Volume 1, Section 7.2.2.1). For example, the average daily minimum air temperature over inland New Guinea Island can warm up to 1°C more than some coastal regions and small islands, while the average daily maximum can warm up to 4°C more.

Interannual variability in surface temperature over Papua New Guinea is strongly influenced by ENSO in the current climate (Section 11.5). As there is no consistency in projections of future ENSO activity (Volume 1, Section 6.4.1), it is not possible to determine whether interannual variability in temperature will change in the future. However, ENSO is expected to continue to be an important source of variability for the region.

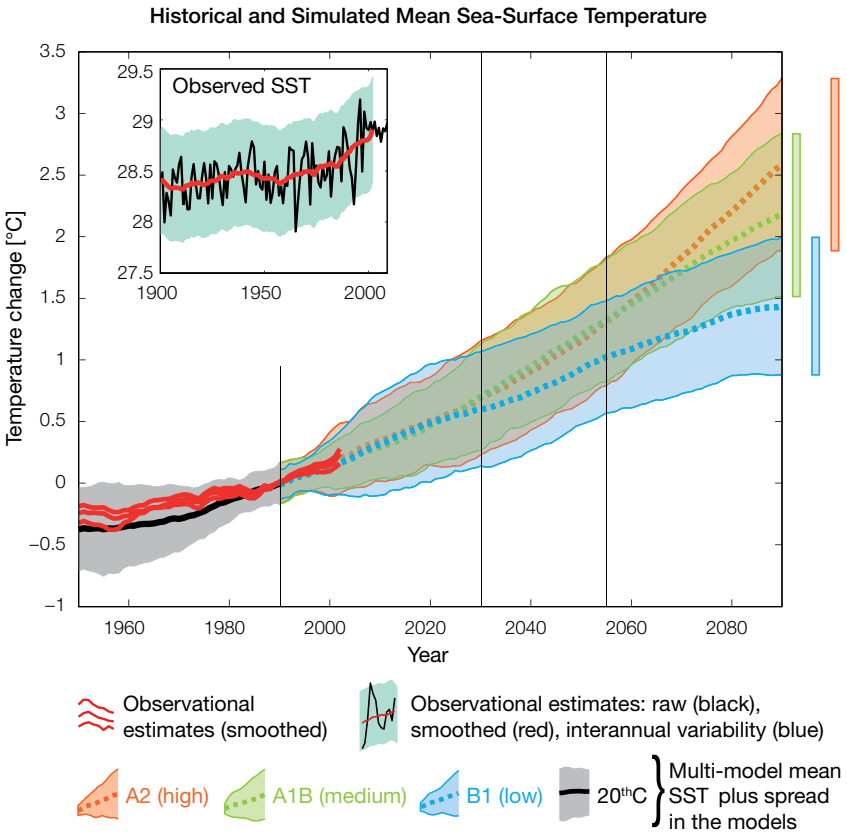

Figure 11.8: Historical climate (from 1950 onwards) and simulated historical and future climate for annual mean sea-surface temperature (SST) in the region surrounding Papua New Guinea, for the CMIP3 models. Shading represents approximately 95% of the range of model projections (twice the inter-model standard deviation), while the solid lines represent the smoothed (20-year running average) multi-model mean temperature. Projections are calculated relative to the 1980–1999 period (which is why there is a decline in the inter-model standard deviation around 1990). This highlights the fact that near-term projections are relatively independent of both model and emissions scenario (although they are significantly affected by natural variability). Observational estimates in the main figure (red lines) are derived from the HadSST2, ERSST and Kaplan Extended SST V2 datasets (Volume 1, Section 2.2.2). Annual average (black) and 20-year running average (red) HadSST2 data is also shown inset.

11.7.2 Rainfall

Wet season (November-April), dry season (May-October) and annual average rainfall are projected to increase over the course of the 21st century. There is *high* confidence in this direction of change because:

- Physical arguments indicate that rainfall will increase in the equatorial Pacific in a warmer climate (IPCC, 2007; Volume 1, Section 6.4.3).
- Almost all of the CMIP3 models agree on this direction of change by 2090.

The CMIP3 models are approximately equally divided between increase (>5%) and little change (-5% to 5%) in annual and seasonal rainfall by 2030, however by 2090 under the higher emissions scenarios (i.e. A2 (high) and A1B (medium)) the majority of the models simulate an increase, with approximately half simulating a large increase (>15%) (Table 11.4). There is *moderate* confidence in this range and distribution of possible futures because:

- In simulations of the current climate, the CMIP3 models broadly capture the influence of the West Pacific Monsoon, Intertropical Convergence Zone and the South Pacific Convergence Zone on the rainfall of Papua New Guinea (Volume 1, Section 5.2.3), although most models produce monsoon westerly winds that do not extend far enough east into the Pacific basin.
- The CMIP3 models are unable to resolve many of the physical processes involved in producing rainfall. As a consequence, they do not simulate rainfall as well as other variables such as temperature (Volume 1, Chapter 5).

The 8 km CCAM simulations indicate considerable spatial variability in rainfall changes across Papua New Guinea associated with the complex topography, with increases in rainfall in some regions and decreases for other regions (Volume 1, Section 7.2.2.1).

These small-scale spatial changes are somewhat correlated with the present day rainfall climatology (e.g. regions that are wettest in the current climate tend to be associated with the highest rainfall increases in the future).

Interannual variability in rainfall over Papua New Guinea is strongly influenced by ENSO in the current climate (Section 11.5). As there is no consistency in projections of future ENSO activity (Volume 1, Section 6.4.1), it is not possible to determine whether interannual variability in rainfall will change in the future.

11.7.3 Extremes

Temperature

The intensity and frequency of days of extreme heat are projected to increase over the course of the 21st century. There is *very high* confidence in this direction of change because:

- An increase in the intensity and frequency of days of extreme heat is physically consistent with rising greenhouse gas concentrations.
- All CMIP3 models agree on the direction of change for both intensity and frequency.

The majority of CMIP3 models simulate an increase of approximately 1°C in the temperature experienced on the 1-in-20-year hot day by 2055 under the B1 (low) emissions scenario, with an increase of over 2.5°C simulated by the majority of models by 2090 under the A2 (high) emissions scenario (Table 11.4). There is *low* confidence in this range and distribution of possible futures because:

- In simulations of the current climate, the CMIP3 models tend to underestimate the intensity and frequency of days of extreme heat (Volume 1, Section 5.2.4).
- Smaller increases in the frequency of days of extreme heat are projected by the CCAM 60 km simulations.

Rainfall

The intensity and frequency of days of extreme rainfall are projected to increase over the course of the 21st century. There is *high* confidence in this direction of change because:

- An increase in the frequency and intensity of extreme rainfall is consistent with larger-scale projections, based on the physical argument that the atmosphere is able to hold more water vapour in a warmer climate (Allen and Ingram, 2002; IPCC, 2007). It is also consistent with physical arguments which indicate that rainfall will increase in the deep tropical Pacific in a warmer climate (IPCC, 2007; Volume 1, Section 6.4.3).
- Almost all of the CMIP3 models agree on this direction of change for both intensity and frequency.

The majority of CMIP3 models simulate an increase of at least 15 mm in the amount of rain received on the 1-in-20-year wet day by 2055 under the B1 (low) emissions scenario, with an increase of at least 30 mm simulated by 2090 under the A2 (high) emissions scenario. The majority of models project that the current 1-in-20-year event will occur, on average, three to four times every year by 2055 under the B1 (low) emissions scenario and six times every year by 2090 under the A2 (high) emissions scenario. There is *low* confidence in this range and distribution of possible futures because:

- In simulations of the current climate, the CMIP3 models tend to underestimate the intensity and frequency of extreme rainfall (Volume 1, Section 5.2.4).
- The CMIP3 models are unable to resolve many of the physical processes involved in producing extreme rainfall.

Drought

The incidence of drought is projected to decrease over the course of the 21st century. There is *moderate* confidence in this direction of change because:

- A decrease in drought is consistent with projections of increased rainfall (Section 11.7.2).
- The majority of models agree on this direction of change for most drought categories.

The majority of CMIP3 models project that mild drought will occur approximately seven to eight times every 20 years in 2030 under all emissions scenarios, decreasing to six to seven times by 2090. The frequency of moderate and severe drought is projected to remain approximately stable, at once to twice and once every 20 years, respectively. There is *low* confidence in this range and distribution of possible futures because:

- There is only moderate confidence in the range of rainfall projections (Section 11.7.2), which directly influences projections of future drought conditions.

Tropical Cyclones

Tropical cyclone numbers are projected to decline in the south-west Pacific Ocean basin (0–40ºS, 130ºE–170ºE) over the course of the 21st century. There is *moderate* confidence in this direction of change because:

- Many studies suggest a decline in tropical cyclone frequency globally (Knutson et al., 2010).
- Tropical cyclone numbers decline in the south-west Pacific Ocean in the majority assessment techniques.

Based on the direct detection methodologies (Curvature Vorticity Parameter (CVP) and the CSIRO Direct Detection Scheme (CDD) described in Volume 1, Section 4.8.2), 55% of projections show no change or a decrease in tropical cyclone formation when applied to the CMIP3 climate models for which suitable output is available. When these techniques are applied to CCAM, 100% of projections show a decrease in tropical cyclone formation. In addition, the Genesis Potential Index (GPI) empirical technique suggests that conditions for tropical cyclone formation will become less favourable in the south-west Pacific Ocean basin, for the majority (80%) of analysed CMIP3 models. There is *moderate* confidence in this range and distribution of possible futures because:

- In simulations of the current climate, the CVP, CDD and GPI methods capture the frequency of tropical cyclone activity reasonably well (Volume 1, Section 5.4).

Despite this projected reduction in total cyclone numbers, five of the six CCAM 60 km simulations show an increase in the proportion of the most severe cyclones. Most models also indicate a reduction in tropical cyclone wind hazard north of 20ºS latitude and regions of increased hazard south of 20ºS latitude. This increase in wind hazard coincides with a poleward shift in the latitude at which tropical cyclones are most intense.

11.7.4 Ocean Acidification

The acidification of the ocean will continue to increase over the course of the 21st century. There is *very high* confidence in this projection as the rate of ocean acidification is driven primarily by the increasing oceanic uptake of carbon dioxide, in response to rising atmospheric carbon dioxide concentrations.

Projections from all analysed CMIP3 models indicate that the annual maximum aragonite saturation state will reach values below 3.5 by about 2040 and continue to decline thereafter (Figure 11.9; Table 11.4). There is *moderate* confidence in this range and distribution of possible futures because the projections are based on climate models without an explicit representation of the carbon cycle and with relatively low resolution and known regional biases.

The impact of acidification change on the health of reef ecosystems is likely to be compounded by other stressors including coral bleaching, storm damage and fishing pressure.

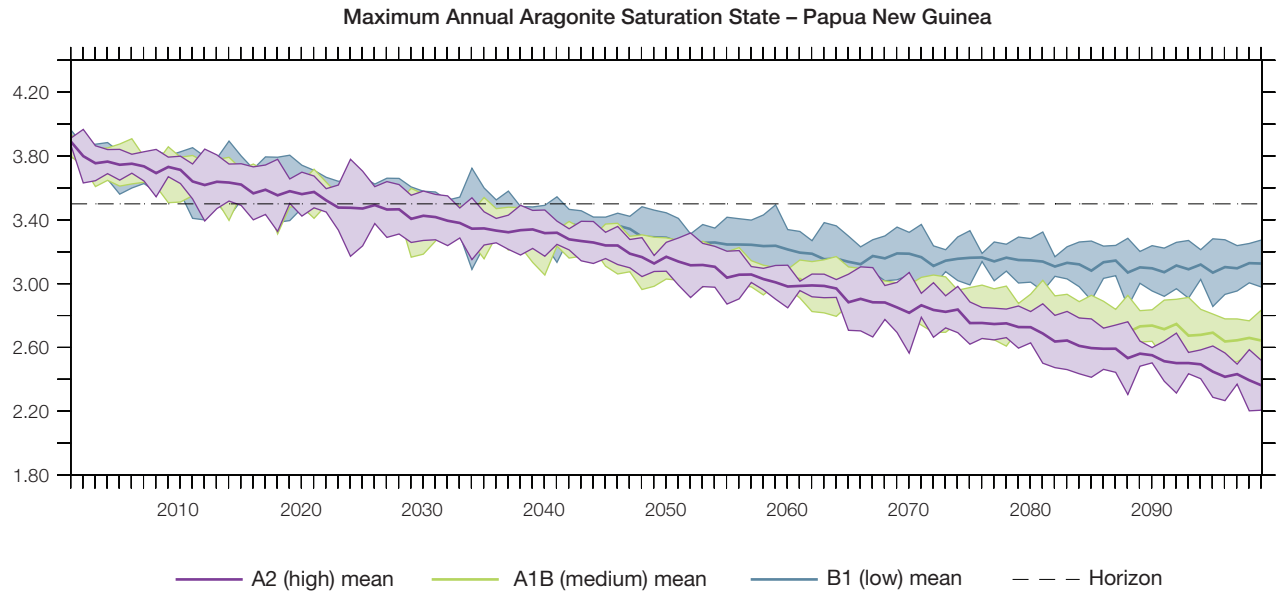

Figure 11.9: Multi-model projections, and their associated uncertainty (shaded area represents two standard deviations), of the maximum annual aragonite saturation state in the sea surface waters of the Papua New Guinea region under the different emissions scenarios. The dashed black line represents an aragonite saturation state of 3.5.

11.7.5 Sea Level

Mean sea level is projected to continue to rise over the course of the 21st century. There is *very high* confidence in this direction of change because:

- Sea-level rise is a physically consistent response to increasing ocean and atmospheric temperatures, due to thermal expansion of the water and the melting of glaciers and ice caps.
- Projections arising from all CMIP3 models agree on this direction of change.

The CMIP3 models simulate a rise of between approximately 5–15 cm by 2030, with increases of 20–60 cm indicated by 2090 under the higher emissions scenarios (i.e. A2 (high) and A1B (medium); Figure 11.10; Table 11.4). There is *moderate* confidence in this range and distribution of possible futures because:

- There is significant uncertainty surrounding ice-sheet contributions to sea-level rise and a rise larger than projected above cannot be excluded (Meehl et al., 2007b). However, understanding of the processes is currently too limited to provide a best estimate or an upper bound (IPCC, 2007).
- Globally, since the early 1990s, sea level has been rising near the upper end of the above projections. During the 21st century, some studies (using semi-empirical models) project faster rates of sea-level rise.

Interannual variability of sea level will lead to periods of lower and higher regional sea levels. In the past, this interannual variability has been about 23 cm (5–95% range, after removal of the seasonal signal; dashed lines in Figure 11.10 (a)) and it is likely that a similar range will continue through the 21st century. In addition, winds and waves associated with weather phenomena will continue to lead to extreme sea-level events.

In addition to the regional variations in sea level associated with ocean and mass changes, there are ongoing changes in relative sea level associated with changes in surface loading over the last glacial cycle (glacial isostatic adjustment) and local tectonic motions. The glacial isostatic motions are relatively small for the PCCSP region.

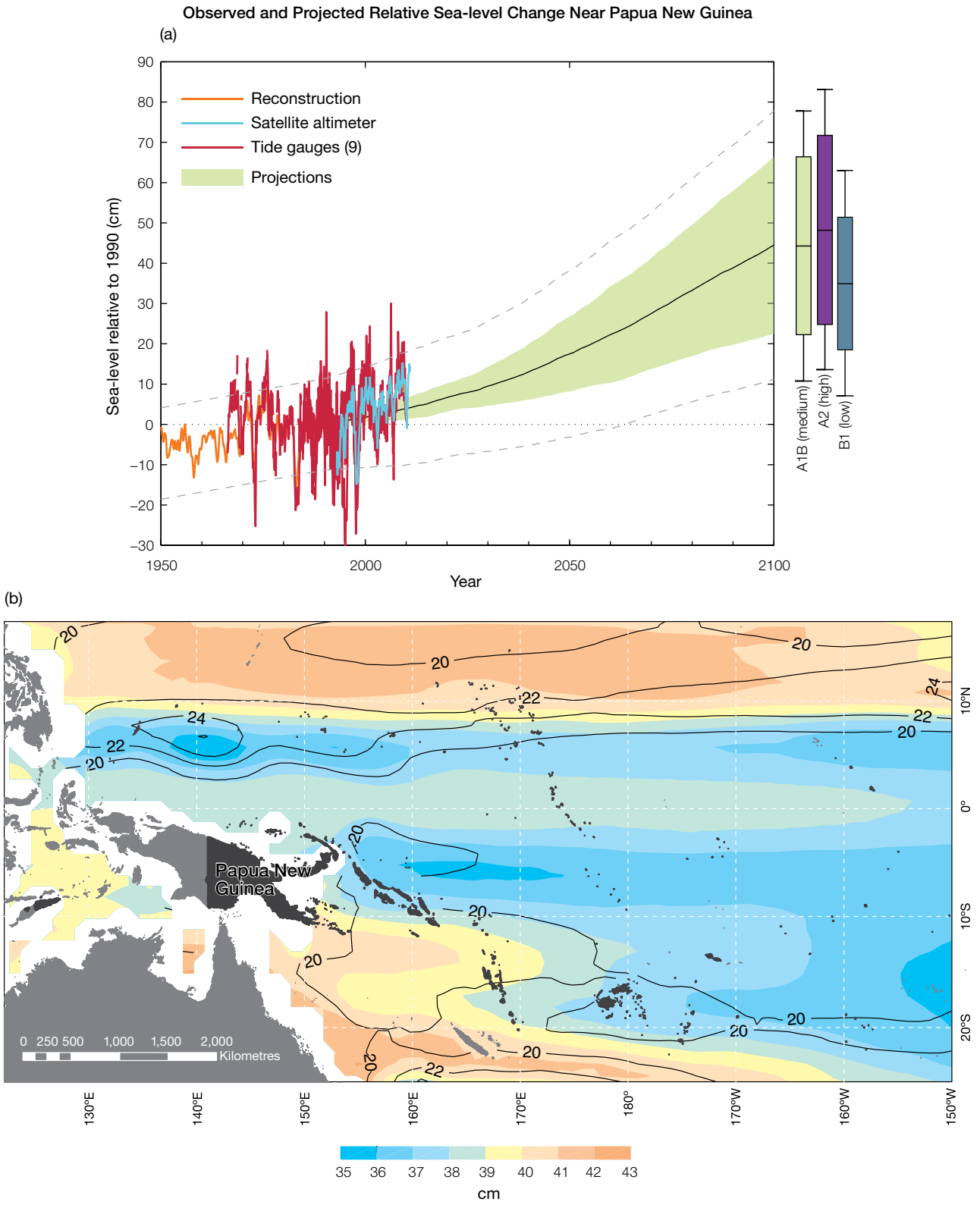

Figure 11.10: Observed and projected relative sea-level change near Papua New Guinea. (a) The observed in situ relative sea-level records are indicated in red, with the satellite record (since 1993) in light blue. The gridded sea level near Papua New Guinea (since 1950, from Church and White (in press)) is shown in orange. The projections for the A1B (medium) emissions scenario (5–95% uncertainty range) are shown by the green shaded region from 1990–2100. The range of projections for the B1 (low), A1B (medium) and A2 (high) emissions scenarios by 2100 are also shown by the bars on the right. The dashed lines are an estimate of interannual variability in sea level (5–95% range about the long-term trends) and indicate that individual monthly averages of sea level can be above or below longer-term averages. (b) The projections (in cm) for the A1B (medium) scenario in the Papua New Guinea region for the average over 2081–2100 relative to 1981–2000 are indicated by the shading, with the estimated uncertainty in the projections indicated by the contours (in cm).

11.7.6 Projections Summary

The projections presented in Section 11.7 are summarised in Table 11.4. For detailed information regarding the various uncertainties associated with the table values, refer to the preceding text in Sections 11.7 and 1.7, in addition to Chapters 5 and 6 in Volume 1. When interpreting the differences between projections for the B1 (low), A1B (medium) and A2 (high) emissions scenarios, it is also important to consider the emissions pathways associated with each scenario (Volume 1, Figure 4.1) and the fact that a slightly different subset of models was available for each (Volume 1, Appendix 1).

Table 11.4: Projected change in the annual and seasonal mean climate for Papua New Guinea, under the B1 (low; blue), A1B (medium; green) and A2 (high; purple) emissions scenarios. Projections are given for three 20-year periods centred on 2030 (2020–2039), 2055 (2046–2065) and 2090 (2080–2099), relative to 1990 (1980–1999). Values represent the multi-model mean change ± twice the inter-model standard deviation (representing approximately 95% of the range of model projections), except for sea level where the estimated mean change and the 5–95% range are given (as they are derived directly from Intergovernmental Panel on Climate Change Fourth Assessment Report values). The confidence (Section 1.7.2) associated with the range and distribution of the projections is also given (indicated by the standard deviation and multi-model mean, respectively). See Volume 1, Appendix 1 for a complete listing of CMIP3 models used to derive these projections.

Variable	Season	2030	2055	2090	Confidence
Surface air temperature (°C)	Annual	+0.7 ± 0.4 +0.8 ± 0.4 +0.7 ± 0.3	+1.1 ± 0.5 +1.5 ± 0.5 +1.5 ± 0.4	+1.6 ± 0.6 +2.4 ± 0.8 +2.8 ± 0.6	High
Maximum temperature (°C)	1-in-20-year event	N/A	+1.0 ± 0.9 +1.4 ± 0.9 +1.5 ± 0.7	+1.3 ± 1.0 +2.2 ± 1.3 +2.7 ± 1.5	Low
Minimum temperature (°C)	1-in-20-year event	N/A	+1.4 ± 1.8 +1.7 ± 2.0 +1.6 ± 1.8	+1.8 ± 1.8 +2.4 ± 1.9 +2.6 ± 2.1	Low
Total rainfall (%)*	Annual	+3 ± 13 +3 ± 13 +5 ± 9	+8 ± 13 +7 ± 17 +7 ± 13	+11 ± 13 +15 ± 20 +15 ± 21	Moderate
Wet season rainfall (%)*	November-April	+4 ± 12 +5 ± 11 +6 ± 10	+10 ± 13 +9 ± 17 +8 ± 12	+12 ± 12 +16 ± 18 +15 ± 20	Moderate
Dry season rainfall (%)*	May-October	+1 ± 15 +1 ± 16 +4 ± 12	+7 ± 16 +5 ± 20 +6 ± 17	+10 ± 16 +15 ± 24 +15 ± 26	Moderate
Sea-surface temperature (°C)	Annual	+0.6 ± 0.5 +0.7 ± 0.4 +0.7 ± 0.5	+1.0 ± 0.5 +1.3 ± 0.5 +1.3 ± 0.5	+1.4 ± 0.6 +2.2 ± 0.7 +2.6 ± 0.7	High
Aragonite saturation state (Ωar)	Annual maximum	+3.5 ± 0.1 +3.4 ± 0.1 +3.4 ± 0.1	+3.2 ± 0.1 +3.0 ± 0.1 +3.0 ± 0.1	+3.1 ± 0.1 +2.7 ± 0.2 +2.5 ± 0.1	Moderate
Mean sea level (cm)	Annual	+9 (4–14) +10 (5–14) +10 (4–15)	+18 (10–26) +20 (9–30) +20 (10–29)	+31 (17–46) +39 (20–58) +41 (22–60)	Moderate

*The MIROC3.2(medres) and MIROC3.2(hires) models were eliminated in calculating the rainfall projections, due to their inability to accurately simulate one or more of the South Pacific Convergence Zone, Intertropical Convergence Zone and the West Pacific Monsoon (Volume 1, Section 5.5.1).